

# 14

## Scanning Probe Microscopy

### 14.1 Introduction

Since the conception of scanning probe microscopy (SPM) in the 1990s, the technique has evolved from a novelty to a **standard analytical tool** in both academic and industrial settings. The number of variations and applications has dramatically escalated over the last ten years. SPM is a fundamentally simple and inexpensive technology that is capable of imaging and measuring surfaces on a fine scale and of altering surfaces at the atomic level. There are **three elements** common to all probe microscopes. Firstly, a small, sharp probe comes within a few tenths of nanometers of the sample's surface, and the interactions between the surface and the probe are used to interrogate the surface. Secondly, a detection system monitors the product of the probe-surface interaction (e.g., a force, tunneling current, change in capacitance, etc.). Thirdly, either the probe or sample is raster-scanned with nanoscale precision. By monitoring of the interaction intensity, any surface variation translates to topographical information from the surface and generates a three-dimensional image of the surface.

Over twenty different variations of the SPM currently exist; however, the most commonly used are Atomic Force Microscopy (AFM) and Scanning Tunneling Microscopy (STM). **In AFM**, the probe tip is affixed to a cantilevered beam (Fig. 14.1). The probe interacts with the surface and the resulting force deflects the beam in a **repulsive manner**, as described by Hooke's Law. In the same manner that a spring changes dimensions under the influence of forces, **the attractive and repulsive forces between atoms of the probe and the surface can also be monitored when brought extremely close to each other**. Hence, the net forces acting on the probe tip deflect the cantilever, and the tip displacement is proportional to the force between the surface and the tip. As the probe tip is scanned across the surface, a laser beam reflects off the cantilever. By monitoring the net ( $x$ ,  $y$ , and  $z$ ) deflection of the cantilever, a three-dimensional image of the surface is constructed. **In STM**, a sharp metallic probe and a conducting sample are brought together until their electronic wave functions overlap (Fig. 14.2). By applying a potential bias between them, a tunneling current is produced. The probe is mounted on a piezoelectric drive that scans the surface. Combination of the piezoelectric drive with a feedback loop allows imaging of the surface in either a **constant-current** or a **constant-height mode**.

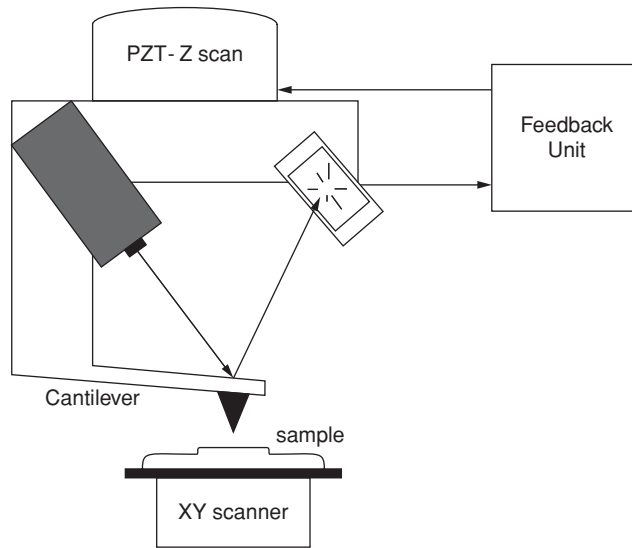


FIGURE 14.1. Schematic of AFM.

Other methods are also utilized to detect the deflection of the cantilever. A plate is placed above the AFM cantilever, which acts as the other plate of a capacitor. The capacitance between the two plates reflects the deflection of the cantilever. Another mode uses laser interferometry, where a beam is split with one part reaching the detector directly while the other part is focused on the back of the cantilever and is reflected back

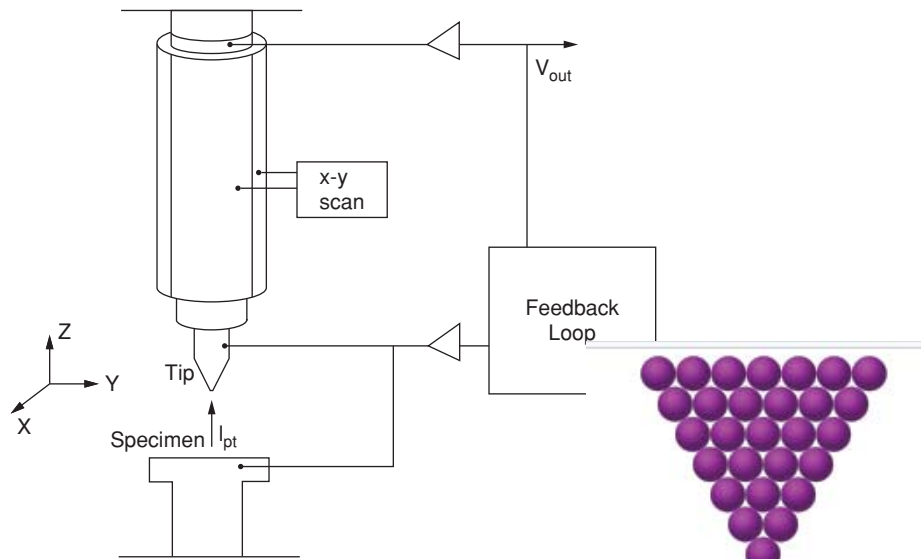
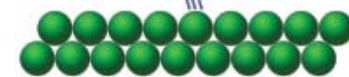


FIGURE 14.2. Schematic of STM.



to the detector. The coherent beams travel different paths and produce an interference pattern, which changes as the cantilever moves up and down. This pattern allows direct imaging of surfaces and defects in real space, with subnanoscale resolution in contrast to diffraction-based analyses. Diffraction analysis samples a macroscopic volume of materials; whereas, SPM can sample small areas ( $<1 \mu\text{m}^2$ ). Operating in the near field, probe–sample spacing is on the order of typical wavelengths used in electron microscopy. Hence, imaging is not diffraction limited and the spatial resolution is not a function of the wavelengths. Ideally, analysis of nanoscale features can be done in vacuum or ambient. In comparison to electron microscopy, the SPM has much lower capital and maintenance costs and essentially no sample preparation.

## 14.2 Scanning Tunneling Microscopy

### 14.2.1 Theory

Scanning tunneling microscopy (STM) has the potential to image the surface of materials. Under carefully controlled conditions, STM has subatomic resolution and is capable of imaging individual atoms and electronic structure. However, analyses using STM are typically limited to electrically conducting materials, since the technique measures a current between the probe tip and the sample surface. The tip of the probe consists ideally of a single atom that comes in close proximity to the surface (Fig. 14.3). In the same manner as a profilometer, the tip is scanned over the surface. However, it does not touch the surface. The separation distance is normally a few tenths of nanometers. This distance allows the wave functions to overlap and results in a finite probability that the electron can surmount the barrier between the probe tip and the sample surface.

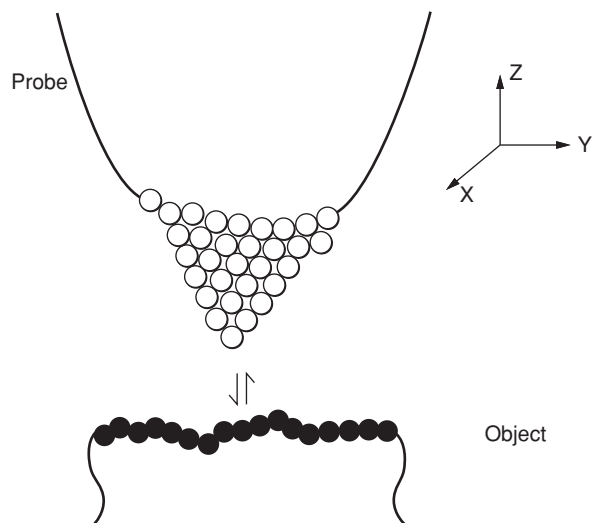


FIGURE 14.3. Schematic showing the interaction between the atoms of the probe tip and the atoms of the sample under interrogation.

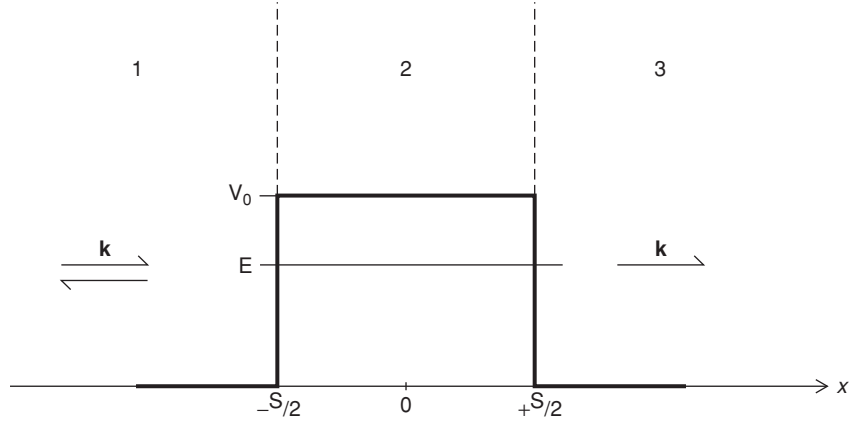


FIGURE 14.4. Schematic of an electron with energy  $E$  impinging upon a one-dimensional rectangular potential barrier of height  $V_0$  and width  $s$ .

Typically, the probe tip is grounded and the sample is biased in the range of tens of millivolts, resulting in a tunneling current. In normal electrical conduction, the two metallic surfaces conduct electricity when they are touching in a contiguous matter. There is, however, a case when the two metallic surfaces (the tip and the sample) are not actually touching and yet a current flows. The current that flows is referred to as a *tunneling current*.

According to **quantum mechanics**, there is a finite probability that the electron can *tunnel* through the barrier, without ever acquiring the full energy (kinetic plus potential energy) necessary to surmount the barrier. Assuming elastic tunneling (the electron does not lose nor gain energy), we consider an electron with energy  $E$  and mass  $m$  impinging upon a one-dimensional barrier with an energy height of  $V_0$  (Fig. 14.4). The electron can be reflected by the barrier (region 1), or tunnel (region 2), or complete the tunneling process (region 3). Starting with Schrödinger's time-independent equation for region 1,

$$-\frac{\hbar^2}{2m} \frac{d^2\psi_1}{dx^2} = E\psi_1,$$

$$\psi_1 = e^{ikx} + Ae^{-ikx}, \quad (14.1)$$

where the wave vector  $k$  is equal to  $[2mE/\hbar^2]^{1/2}$  and  $\hbar$  is Plank's constant divided by  $2\pi$ . In region 2, the wave function relationship is described as

$$-\frac{\hbar^2}{2m} \frac{d^2\psi_2}{dx^2} + V_0 = E\psi_2,$$

$$\psi_2 = B'e^{ikx} + C'e^{-ikx} = Be^{-\xi x} + Ce^{-i\xi x}, \quad (14.2)$$

where, in this case,  $\xi$  is equal to  $[-k'^2]^{1/2} = [2m(V_0 - E)/\hbar^2]^{1/2}$ . Finally in region 3,

$$-\frac{\hbar^2}{2m} \frac{d^2\psi_3}{dx^2} = E\psi_3,$$

$$\psi_3 = De^{ikx}. \quad (14.3)$$

The incident current density  $j_i$  and transmitted current density  $j_t$  are given (Wiesendagner, 1994) as

$$\begin{aligned} j_i &= \frac{-i\hbar}{m} \left( \psi_3^*(x) \frac{d\psi_3}{dx} - \psi_3(x) \frac{d\psi_3^*}{dx} \right), \\ j_i &= \frac{-i\hbar}{m} |D|^2, \\ j_t &= \frac{\hbar k}{m}. \end{aligned} \quad (14.4)$$

By matching the wave functions  $\psi_j$  and the corresponding first derivatives at the edges of the barriers,  $x = 0$  and  $x = s$  (discontinuities in the potential), the transmission coefficient  $T$ , the ratio of current density  $j_t$  and incident current  $j_i$  are determined:

$$\begin{aligned} T &= \frac{j_t}{j_i} = |D|^2 \\ &= \frac{1}{1 + (k^2 + \xi^2)^2 / (4k^2\xi^2) \sinh^2(\xi s)} \\ &\approx \frac{16k^2\xi^2}{(K^2 + \xi^2)^2} \exp(-2\xi s), \end{aligned} \quad (14.5)$$

where the term  $\xi$  equals  $[2m(V_0 - E)]^{1/2}/\hbar$  and is referred to as the *decay rate*. Hence, the **effective barrier height**  $\phi (= V_0 - E)$  and the barrier width  $s$  dictate the tunneling current. For the case of the tunneling microscope, where the gap between the sample and probe is **0.1 nm**, any small bias applied between the probe tip and sample will generate a large electrostatic field. An approximation of the magnitude of the tunneling current ( $I$ ) is an exponential function of the separation distance between the probe tip and the sample:

$$I = C \rho_s \rho_t \exp\left(s\phi^{1/2}\right) \quad (14.6)$$

where  $\rho_s$  and  $\rho_t$  are the electron densities of the sample surface and probe tip, respectively.  $C$  is proportionately constant, the probe tip scans across the surface using a **piezoelectric crystal** that changes its volume when a voltage is applied to it. **As the tip moves in the  $x$ - or  $y$ -direction along the sample's surface, the current varies according to Eq. 14.6.** The output current differs when the probe tip is right on top of an atom (smaller distance) as compared to when the probe tip is above a space between atoms (larger distance). Hence, the relative electrostatic potential of an individual atom is detected as an increase in the tunneling current as a function of spatial position in the  $x$ - $y$  scan across the sample's surface. For case where the  $\phi$  equals 5 eV, a variation in  $s$  from 0.1 to 1.0 nm results in a variation in tunneling current by a factor of 7.5.

In Fig. 14.5a, the actual probe-tip-surface displacement,  $s$ , is held constant, and is the constant-height mode of operation. Consequently, the output current varies with the electron density. Monitoring of the probe current as a function of the  $x$ - $y$  displacement yields a topographical representation of the surface morphology. On the basis of Eq. 14.6, this mode of operation is sensitive to small fluctuations in  $s$  and results in an exponential increase or decrease in output current.

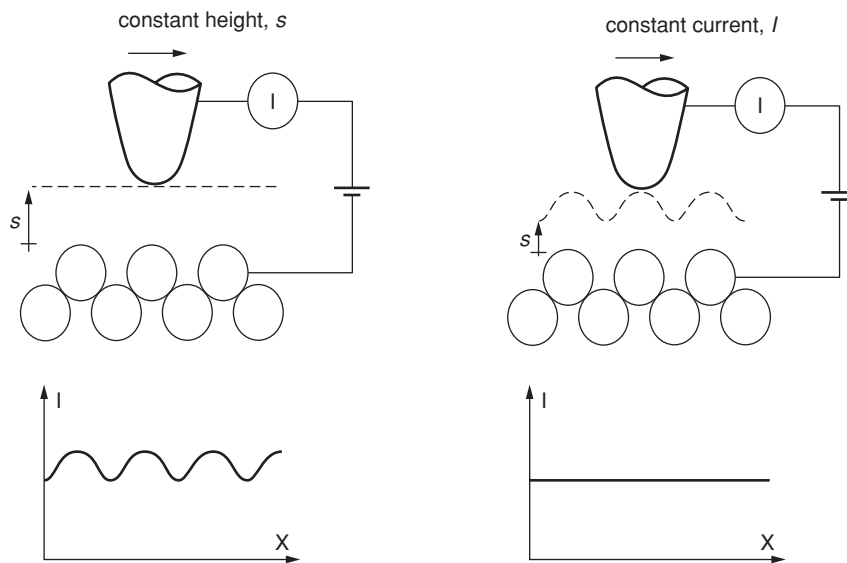


FIGURE 14.5. Schematic of STM probe tip scanning in the  $x$ -direction when operating in (a) constant-height mode and (b) constant-current mode.

Often it is desired that the output signal vary linearly with the probe-tip surface displacement,  $s$ . In this case, a feedback loop is employed in *constant-current mode*, which controls the height of the probe-tip–specimen separation,  $s$  (Fig. 14.5b). The height of the probe tip is controlled by a piezoelectric crystal, a material which expands linearly when a voltage is placed across it. The expanding crystal pushes the tip closer to the sample. Hence, the voltage needed to expand the piezoelectric crystal to keep the current constant varies linearly with the actual height of the atoms on the sample. By monitoring the feedback voltage, we can directly measure the displacement of the tip.

Typical STM analyses are conducted in **ultrahigh vacuum** to minimize contamination. Fig. 14.6a displays a negative-bias ( $-1.06$  V) STM image of a Si(111)  $7 \times 7$  surface. The area of the image is approximately  $24$  nm  $\times$   $24$  nm. Note that the terrace at the kinked edge is clearly visible with atomic resolution. In the accompanying Fig. 14.6b, the high-resolution STM image is taken with a negative bias of ( $-0.12$  V). The line denotes the asymmetry of the faulted and unfaulted halves of the  $7 \times 7$  unit cell. With low-bias voltage ( $-0.12$  V), the adatoms in the faulted region gives rise to more tunneling current than the matrix atoms in the unfaulted region. Figure 14.7 shows **UHV-STM** of Quasi-1D gold wires grown on a Si(557) surface taken using a  $1.66$  V bias. The Si(557) surface can be regarded as a combination of Si(111) terraces and single height steps; hence, the Au atoms adsorb to the (111) terraces, forming quasi-one-dimensional gold wires.

Another application of STM is the **manipulation of atoms**. Figure 14.8 shows the formation of a *quantum dot corral*. In this case, Fe atoms are adsorbed onto a Cu(111) surface at a temperature of approximately  $4$ K. The STM probe tip descends directly on

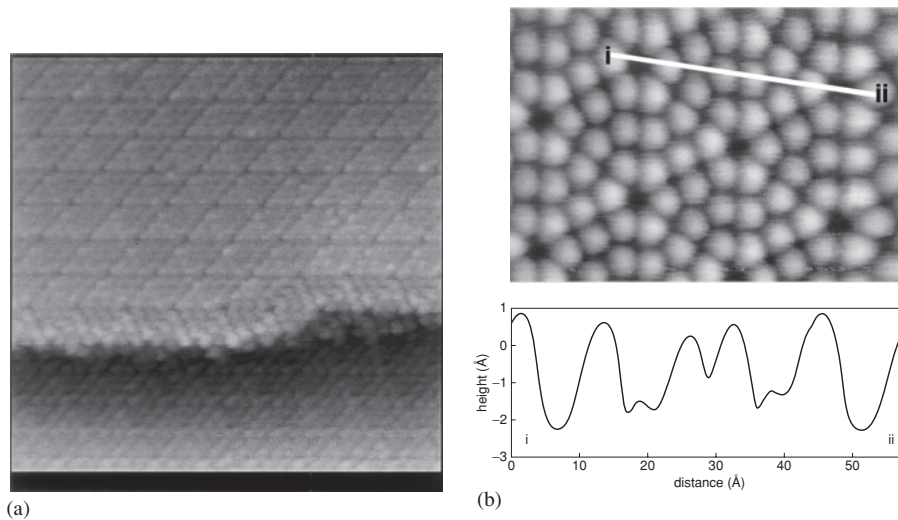


FIGURE 14.6. (a) Constant-height STM image of a Si(111)  $7 \times 7$  surface from an area of  $24 \times 24$  nm. (b) The high-resolution STM image is taken with a negative bias ( $-0.12$  V). The line scan denotes the asymmetry between the faulted and unfaulted regions. [From J.M. Macleod et al., *Review of Scientific Instruments*, Vol. 74, pp. 2429–2437]

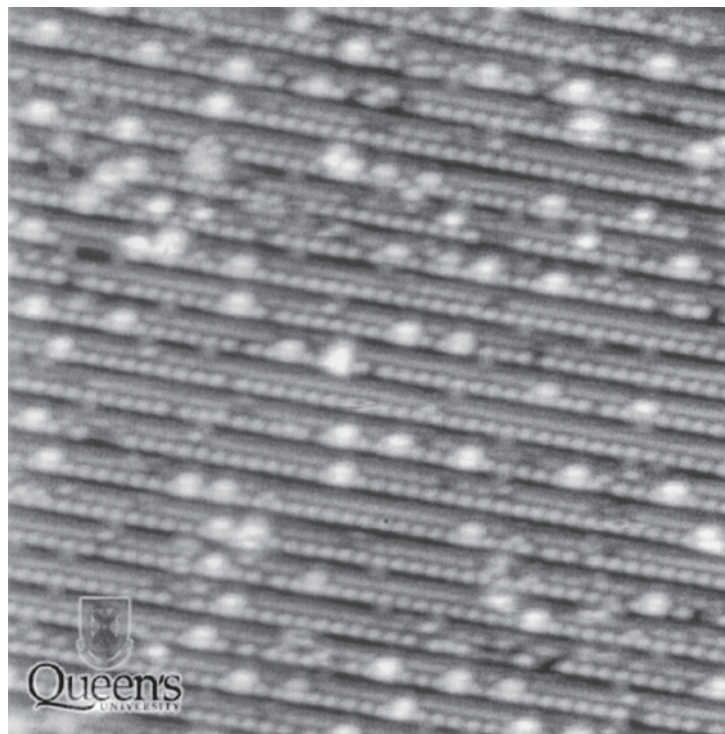


FIGURE 14.7. UHV-STM of Quasi-1D gold wires grown on a Si(557) surface taken using a 1.66 V bias. Au atoms adsorb to the (111) terrace. (With permission from A. McLean, J. Macleod, and J. Lipton-Duffin.)

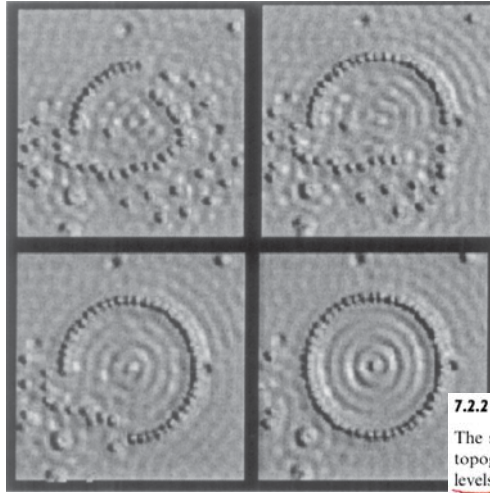


FIGURE 14.8. Series of images displaying the formation of a quantum dot corral using the STM. Fe atoms are adsorbed onto a Cu(111) surface and positioned using the STM. [Image reproduced by permission of IBM Research, Almaden Research Center. Unauthorized use not permitted.]

### 7.2.2 STM spectroscopy

The scanning tunnelling microscope can be used not only simply to map the topography of a sample surface but also to investigate the electronic energy levels at any point on that surface. In the best circumstances, therefore, the nature and state of a single atom can be investigated. This type of spectroscopy is done by varying the potential between the STM tip and the specimen. Figure

top of a Fe atom and increases the attractive force by increasing the tunneling current. The probe tip translates across the surface to the appropriate locale with the tethered Fe atom. Once the appropriate position is determined, the Fe atom is untethered by reducing the tunneling current.

## 14.3 Atomic Force Microscopy

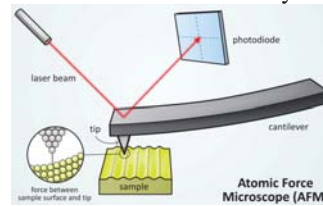
### 14.3.1 Theory

When the probe–surface spacing is relatively large ( $\sim 1$  nm or greater), the interactions are dominated by long-range van der Waals forces (Fig. 14.9). These attractive forces depend exponentially on distance and are extremely sensitive to probe-tip shape. Other attractive forces include metallic adhesion forces and charge accumulation between the probe tip and the nearest surface atom. At small spatial separations ( $\sim 0.1$  nm or less), the wave function of the probe–surface overlap and short-range quantum-mechanical exchange–correlation forces dominate due to the Pauli exclusion principle. These forces decay exponentially with increasing distance:

$$F = -\gamma(\Delta\varepsilon_C)\chi \left( \sigma \frac{H}{e^2} \right)^{1/2}, \quad (14.7)$$

where  $\Delta\varepsilon_C$  is the width of the conduction band,  $\gamma$  is a dimensionless factor approximately equal to one,  $\chi$  is the decay rate of the force, and  $\sigma$  is the conductance.

The slope of the van der Waals curve is very steep in the repulsive or contact region (Fig. 14.9). As a result, the repulsive van der Waals force balances almost any force that attempts to push the atoms closer together. For example, in AFM, when the cantilever pushes the tip against the sample, the cantilever deforms as opposed to pressing the probe tip closer to the surface. Only negligible reduction in the interatomic separation between the probe-tip atom and the surface atoms is probable, even with the use of





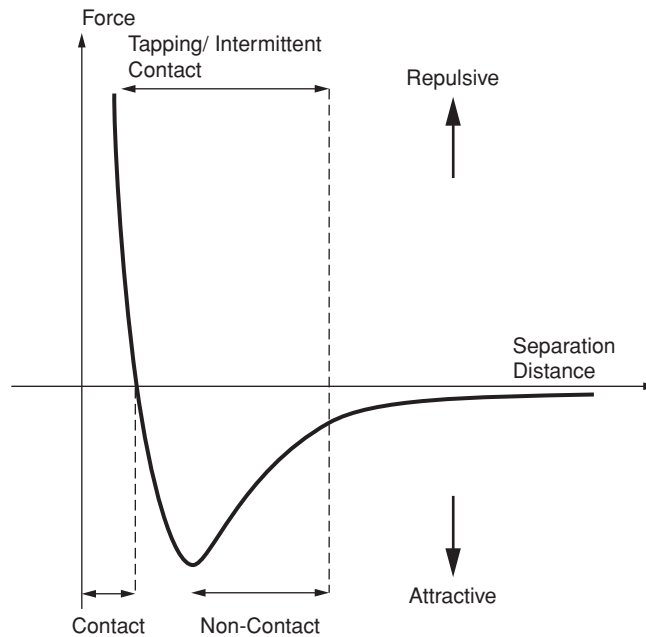


FIGURE 14.9. Schematic of van der Waals forces as a function of probe-tip-surface spacing.

a rigid cantilever. These cantilevers will apply substantial forces onto the sample's surface and will more than likely result in surface deformation. The point of balance between attractive and repulsive forces is defined as the *mechanical point contact*. Van der Waals forces also dominate the interaction between nonmagnetic and electrically natural solids that are separated by a distance of several nanometers.

In addition to the repulsive **van der Waals force** described above, two **other forces** are generally present during contact AFM operation: a **capillary force** exerted by the thin water layer often present in an ambient environment, and the force exerted by the cantilever itself. The capillary force arises when water wicks its way around the tip, applying a strong attractive force (about  $10^{-8}\text{N}$ ) that holds the tip in contact with the surface. As long as the tip is in contact with the sample, the capillary force should be constant because the distance between the tip and the sample is virtually incompressible. It is also assumed that the water layer is reasonably homogeneous. The variable force in contact AFM is the force exerted by the cantilever. The total force that the tip exerts on the sample is the sum of the capillary plus cantilever forces, and must be balanced by the repulsive van der Waals force for contact AFM. The magnitude of the total force exerted on the sample varies from  $10^{-8}\text{N}$  (with the cantilever pulling away from the sample almost as hard as the water is pulling down the tip) to the more typical operating range of  $10^{-7}$  to  $10^{-6}\text{N}$ .

The atomic force microscope (AFM) or scanning force microscope (SFM), like all other scanning probe microscopes, utilizes a sharp probe moving over the surface of a sample in a raster scan (see Fig. 14.1). In the case of the AFM, the probe is a tip on the end of a cantilever that bends in response to the force between the tip and the sample.

An optical detector monitors the extent of bending of the lever. The cantilever beam obeys Hooke's Law for small displacements, and the interaction force between the tip and the sample can be found. The movement of the tip or sample is performed by an extremely precise positioning device made from piezoelectric ceramics. The scanner is capable of subnanometer resolution in the  $x$ -,  $y$ - and  $z$ -directions.

### 14.3.2 Modes of Operation

The AFM typically operates in either of two principal modes: *constant-force mode* (with feedback control) and *constant-height mode* (without feedback control). If the electronic feedback is engaged, then the probe-tip positioning is controlled by the piezoelectric device, which moves the sample (or tip) up and down and responds to any changes in force that are detected, altering the tip-sample separation to restore the force to a predetermined value (similar to Fig. 14.5a). This mode of operation is known as *constant force* and usually results in *accurate topographical images*. In constant-force mode, the speed of scanning is limited by the response time of the feedback circuit, but the total force exerted on the sample by the tip is well controlled (similar to Fig. 14.5b). *Constant-force mode is generally preferred for most applications.*

*Constant-height or deflection mode* operates with the feedback electronics minimized. This mode is particularly practical *for imaging very flat samples* at high resolution. The minimized feedback eliminates issues of thermal drift or the possibility of a rough sample damaging the tip and/or cantilever. Constant-height mode is often used for taking atomic-scale images of atomically flat surfaces, where the cantilever deflections and thus variations in applied force are small. Constant-height mode is also essential for recording real-time *images of changing surfaces*, where high scan speed is essential.

Once the AFM has detected the cantilever deflection, it can generate the topographic data set by operating in one of the two modes—constant-height or constant-force mode. In constant-height mode, the spatial variation of the cantilever deflection can be used directly to generate the topographic data set because the height of the scanner is fixed as it scans. In constant-force mode, the deflection of the cantilever can be used as input to a feedback circuit that moves the scanner up and down in the  $z$ -axis, responding to the topography by keeping the cantilever deflection constant. In this case, the image is generated from the scanner's motion. With the cantilever deflection held constant, the total force applied to the sample is constant.

### 14.3.3 Probe-Sample Interaction

The way in which image contrast is obtained can be achieved in many ways. The three main classes of interaction are *contact mode*, *tapping mode*, and *noncontact mode*. *Contact mode is the most common method of operation of the AFM.* In this case, the tip and sample reside in the repulsive region of Fig. 14.5 during the scan. A consequence of contact-mode operation is that large lateral forces on the sample surface have a tendency to drag the probe tip.

In the *noncontact mode*, the probe tip resonates at a distance above the sample surface of the sample such that it is no longer in the repulsive region of Fig. 14.5. If noncontact

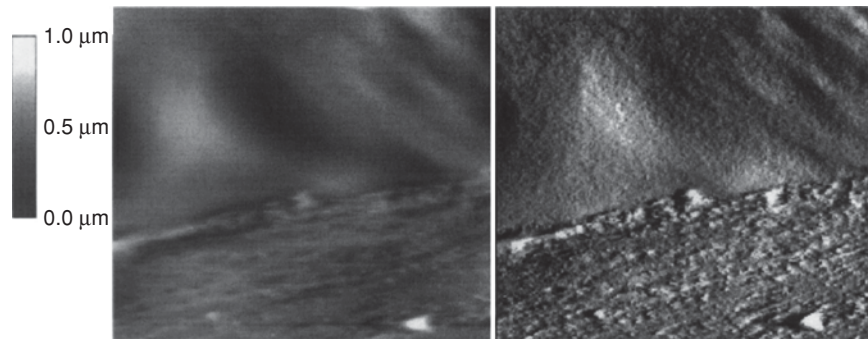


FIGURE 14.10. Image of a piece of mica using AFM (a) in noncontact mode and (b) in contact mode. Note that in this case the contact mode provides more details. [From Le Grimmeléc et al., *Biophys. J.*, 75, 695–703 (1998). With permission of The Biophysical Society.]

mode is used, it is advantageous to conduct the analysis in vacuum. Conducting the analysis in ambient conditions usually results in a thin layer of water contamination between the probe tip and the surface. Fig. 14.10 (a and b) shows a comparison of noncontact- and contact-mode imaging for a piece of mica. In this case, the contact mode provides more details; however, the noncontact mode minimizes risk of damage to the probe tip. Recent advancements have led to the development of a high-resolution,

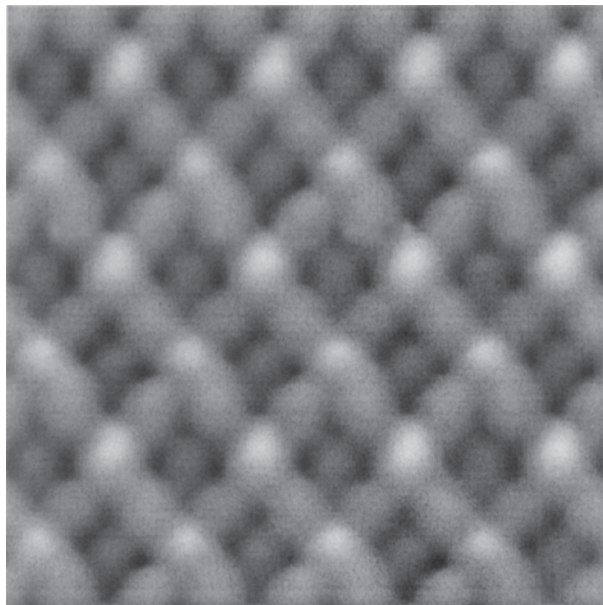


FIGURE 14.11. High resolution, noncontact AFM image taken of the Ge/Si(105) surface. The size of image is 4.2 nm  $\times$  4.2 nm. The frequency shift was set at  $-60$  Hz. The oscillation amplitude and resonant frequency of the cantilever were 3.8 nm and 280 482 Hz, respectively (with permission from Yukio Hasegawa).

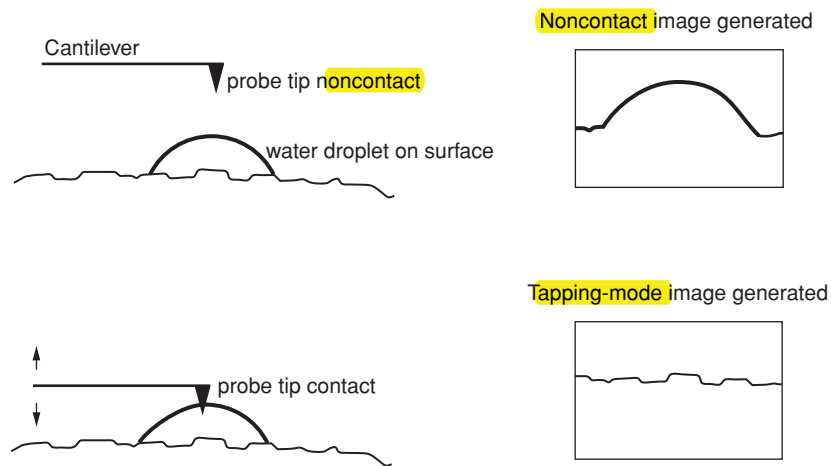


FIGURE 14.12. (a) Schematic displaying the consequence of adsorbed moisture from the ambient during AFM analysis. (b) Tapping-mode AFM is used to avoid the false image of the surface.

atomically resolved electrostatic potential profile, with use of an AFM equipped with a Kelvin probe. Figure 14.11 shows a noncontact AFM micrograph of Ge atoms residing on a Si(105) substrate. The image reveals the electrostatic potential variations among the dangling bond states and all dangling bonds of the surface, regardless of their electronic configuration. These results clearly demonstrate that high-resolution noncontact AFM with a Kelvin-probe method is a tool for imaging atomic structures and determining electronic properties of surfaces. The resolution and results are on a par with or better than STM, whose images strongly deviate from the atomic structure by the electronic states involved.

Figure 14.12a shows the consequence of water contamination on the resulting image during AFM. The presence of the moisture from the ambient adsorbs on the surface and can give a false image. To avoid this problem, tapping mode is the commonly employed mode when operating in air or other gases (Figure 14.12b). In this case, the cantilever resonates at its resonant frequency on the order of 100–400 kilohertz. The probe tip contacts the surface only during a fraction of the resonant period as a means to reduce the influence of the lateral forces on the probe tip. The feedback controls adjust such that the amplitude of the cantilever resonates at a constant value. An image can be formed from this amplitude signal, as there will be small variations in this oscillation amplitude due to the control electronics not responding instantaneously to changes on the specimen surface. This mode eliminates lateral forces between the tip and the sample and has become an important SPM technique, since it overcomes some of the limitations of both contact and noncontact AFM. In the example below, tapping-mode AFM was used to compare the surface morphology of as-deposited and plasma-treated parylene surfaces (Fig. 14.13). AFM results, taken in ambient, reveal the increased surface roughness associated with the oxygen plasma treatment and correlated with mechanical adhesion analysis.

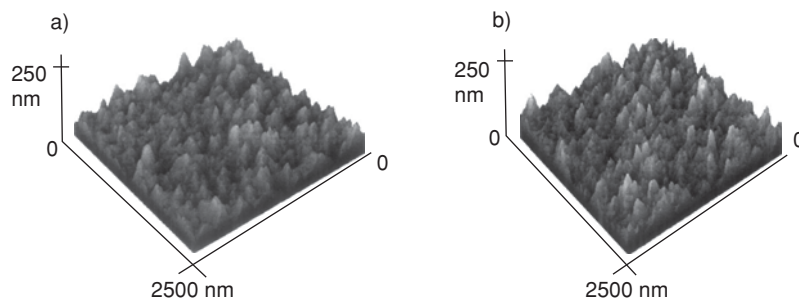


FIGURE 14.13. AFM images of Pa-n on Si: (a) untreated, as-deposited Pa-n on Si, and (b) oxygen plasma-treated Pa-n. Both images were taken in ambient using tapping mode.

#### 14.3.4 Tip Effects

Image contrast using the AFM results from **interaction forces between the probe tip and sample**. Understanding of the probe-tip feature then becomes important for interpretation of the image. During analyses at high magnification and on surfaces with substantial surface morphology, **the probe condition influences the image resolution**. A given feature may be alleged to be topographical that is actually a direct result of the probe-tip shape. **For example, for the probe to interact with individual atoms, these interactions must be limited to the fewest number of atoms on the probe tip. Hence, the resolution of the AFM probe tip depends on the sharpness of the tip**. Commercially fabricated probe tips have a radius of curvature on the order of 10 nm. Sharper (i.e., better) tips are also available. Only a tip with sufficient sharpness can properly image a given Z-gradient. Some gradients will be steeper or sharper than any tip can be expected to image without artifact. Figure 14.14 shows AFM images using a 40 nm diameter probe tip (a) and a 5 nm diameter probe tip (b). **Another effect is tip broadening**, which arises when the tip's radius of curvature is on the order of or larger than the feature under investigation. When the probe tip scans over the specimen, the sides of the tip

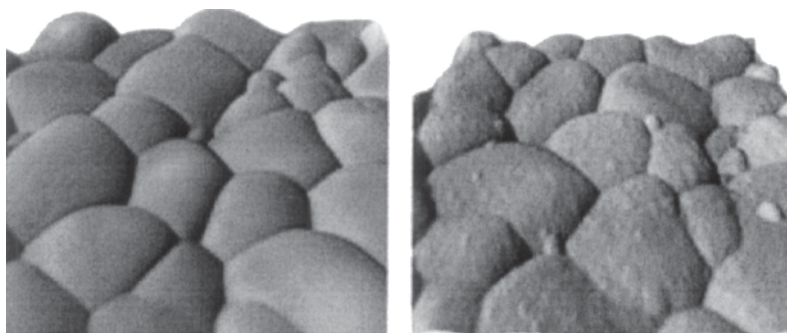


FIGURE 14.14. AFM images using a 40 nm diameter probe tip (a) and a 5 nm diameter probe tip (b). [Courtesy of Paul E. West, Ph.D, CTO, Pacific NanoTechnology.]

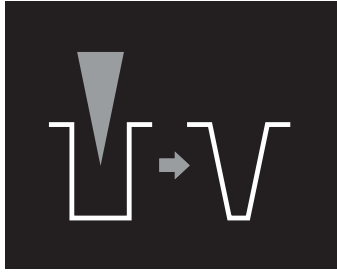


FIGURE 14.15. Schematic of the apparent change in the image of a square hole to a slope-edged hole because of the shape of the probe.

make contact before the base, and the microscope produces a self-image of the probe tip (a false image), rather than of the object surface (see Fig. 14.15).

### *References*

1. R. Wiesendanger, *Scanning Probe Microscopy and Spectroscopy* (Cambridge University Press, New York, 1994).
2. D. A. Bonnell, Ed., *Scanning Tunneling Microscopy and Spectroscopy* (VCH Publishers, New York, 1993).
3. C. Kittel, *Introduction to Solid State Physics*, 5th ed. (John Wiley and Sons, New York, 1976).